Study of the influence of actin-binding proteins using linear analyses of cell deformability

Gustavo R. Plaza, Taro Q. P. Uyeda, Zahra Mirzaei and Craig A. Simmons

The actin cytoskeleton plays a key role in the deformability of the cell and in mechanosensing. Here we analyze the contributions of three major actin cross-linking proteins, myosin II, α-actinin and filamin, to cell deformability, by using micropipette aspiration of *Dictyostelium* cells. We examine the applicability of three simple mechanical models: for small deformation, linear viscoelasticity and drop of liquid with a tense cortex; and for large deformation, a Newtonian viscous fluid. For these models, we have derived linearized equations and we provide a novel, straightforward methodology to analyze the experiments. This methodology allowed us to differentiate the effects of the cross-linking proteins in the different regimes of deformation. Our results confirm some previous observations and suggest important relations between the molecular characteristics of the actin-binding proteins and the cell behavior: the effect of myosin is explained in terms of the relation between the lifetime of the bond to actin and the resistive force; the presence of α-actinin obstructs the deformation of the cytoskeleton, presumably mainly due to the higher molecular stiffness and to the lower dissociation rate constants; and filamin contributes critically to the global connectivity of the network, possibly by rapidly turning over cross-links during the remodeling of the cytoskeletal network, thanks to the higher rate constants, flexibility and larger size. The results suggest a sophisticated relationship between the expression levels of actin-binding proteins, deformability and mechanosensing.

Introduction

The mechanical properties of living cells are of interest in order to understand their response to deformation, their ability to migrate, their mechanosensing capabilities and their contribution to the mechanical properties of tissues. Moreover, by measuring the response of cells to mechanical deformation we can obtain information about the internal structure and the alterations produced by mechanical and chemical stimuli.

Biophysical studies of cells have allowed us to accumulate an impressive amount of information regarding cellular material mechanics. Typically, to measure the mechanical properties of cells, a known force or stress is applied and the resulting deformation is measured.[1–3] Different techniques are used, including atomic force microscopy (AFM), optical trapping (laser tweezers), magnetic beads or micropipette aspiration. Fluorescence microscopy and electron microscopy have contributed to showing the distribution of the different molecules inside the cell, and different mechanical testing techniques have allowed the description of different aspects of the behavior of molecules, organelles, assemblies and the whole cell.

A number of components in cells contribute to their mechanical behavior. For example, the cytosol, the organelles and the nucleus of a cell may have different mechanical properties contributing differently to the global stiffness. In fact, the stiffness of the nucleus is one order of magnitude higher than the stiffness of the whole cell.[4] Depending on the conditions, the cytoplasm may be more or less deformable, approaching viscous-liquid or alternatively viscous-solid behaviour.[5]

The actin cytoskeleton is denser in the cortical region of animal cells. Due to the activity of molecular motors, mainly non-muscle myosin II and also myosin I, the cytoskeleton behaves as an active network with contractile properties. It is assumed that the actomyosin cortex produces a cortical tension that balances the pressure difference between the cytoplasm and the extracellular medium. This mechanism allows equilibration of the pressure difference of osmotic origin.[6] Although the actin filaments and myosin motors are central components,

their behavior is determined by the large number of actin-binding proteins (ABPs). In a cell at rest, molecular fluctuations within the cytoskeletal actin network are governed by the activity of the ABPs that cross-link actin filaments, in particular the motor proteins dependent on the hydrolysis of ATP[7] and the passive cross-linkers such as α-actinin and filamin. The influence of the different ABPs on the mechanical response has been studied using different strategies, particularly studying reconstituted systems of actin and one of several proteins, or mutant cells lacking one or several ABPs. However, due to the complexity of the cytoskeleton, the understanding of the different contributions of each component is only partial.

In this work, we were interested in using simple mechanical models for the cell as a whole, ignoring the above-mentioned details. Therefore we used three simple models and obtained linearized equations to analyze the results. The different assumptions of mechanical descriptions of the cell lead to the calculation of different parameters from the mechanical tests. For small deformations, the cell behavior is solid-like[2,3,5] and a first simple approach is to consider that the cell behaves as a homogeneous material, typically an elastic or viscoelastic solid.[8–13] Mechanical tests allow estimation of the elastic modulus or the viscoelastic parameters when considering the effect of time, or even the complex elastic modulus from dynamic tests. The viscoelastic standard linear solid (a three-parameter model) is considered in this work.

The contractile activity of the cytoskeleton has led, for cells in suspension, to the simplistic model of a drop of liquid with surface tension, or cortical tension, maintained by the contractile actomyosin cortex. Therefore, a second possibility is to model the cell as a drop of liquid with a relatively thin actomyosin cortex bearing constant tension. In the case of micropipette aspiration, the cortical tension is measured by suctioning the surface of the cell and measuring the radii of the membrane, inside and outside the micropipette (estimating the cortical tension in neutrophils, Zhelev *et al.*[14] found that a cortex thickness of 0.3–0.7 μm was required to explain their mechanical measurements by micropipette aspiration; at that moment they did not know the biomolecular origin of the cortex tension). The influence of the ABPs on the cortical tension has also been studied previously by using micropipette aspiration.[15–17]

The homogeneous material model and the liquid drop with cortical tension model are both approximations to the more complex actual microstructure of the cell and can be applied to small deformations. For large deformations, the cytoskeleton behaves as a fluid-like material.[5,18] The third simple approach, used in this work to model the cell-material flow, is to consider a Newtonian fluid with constant viscosity.[19–22]

The aim of this work is to analyze the effect of ABPs by applying the three above-mentioned simple models, analyzing the consequences of the lack of either of the two major passive actin cross-linking proteins or myosin II in the cellular slime mold *Dictyostelium discoideum*. We tested the cells by micropipette aspiration up to large deformation and observed the evolution of the shape over time. Our results may be related to previous studies on the effect of stress on the distribution of ABPs.[17,23]

Mechanical models

In this section we describe briefly the simple mechanical models used in this work and explain the derivation of the three equations used to estimate the viscoelastic parameters (eqn (9)), the cortical tension (eqn (12)) and the apparent viscosity of the cells (eqn (14)). Regarding these models, our objective is to present a simplified approach, measuring properties of the cell as a whole and allowing quantitative comparison of the properties of different cells lines. Therefore the cell is modeled as a homogeneous material, without separating the contributions of the internal components. In this approach we assume linearized expressions for the small deformation regime.

For small deformation, it is customarily observed that the stress in a material is proportional to the strain. We say then that it behaves as a Hookean material or a linear elastic material. For an isotropic homogeneous material with such behavior, in simple tension or compression tests, the ratio between stress σ and strain ε is the Elastic modulus, or Young's modulus, $E = \sigma/\varepsilon$. The neo-Hookean model is the extension of the previous one for larger deformation and incompressible material: for small deformation the neo-Hookean material concurs with a linear elastic material with elastic modulus E.

When time is important, as is the case in soft matter, the ratio between stress and strain is not constant and we use the adjective viscous. Again, for small deformation the mechanical behavior may be considered linear. Then, in a uniaxial relaxation test, *i.e.* when the material is subjected to a constant strain ε_0 from an instant $t = 0$, the ratio between stress $\sigma(t)$ and strain is given by the relaxation modulus $E(t) = \sigma(t)/\varepsilon_0$. In the standard linear solid model, the relaxation modulus depends on three parameters and is given by

$$E(t) = E_{\text{inf}} + (E_0 - E_{\text{inf}})\mathrm{e}^{-t/\tau_{\text{R}}} = E_0[1 - \alpha_1(1 - \mathrm{e}^{-t/\tau_{\text{R}}})], \quad (1a)$$

where E_0 is the initial elastic modulus (at $t = 0$), α_1 is a dimensionless coefficient, $E_{\text{inf}} = E_0(1 - \alpha_1)$ is the elastic modulus at infinite time, and τ_{R} is the relaxation time. Complementarily, in a uniaxial creep test, *i.e.* when the material is subjected to a constant stress σ_0 from an instant $t = 0$, the ratio between strain $\varepsilon(t)$ and stress is given by the creep compliance $J(t) = \varepsilon(t)/\sigma_0$. In the standard linear solid model, this function is given by

$$J(t) = \frac{1 - \alpha_1 \mathrm{e}^{-t/\tau}}{E_0(1 - \alpha_1)}, \quad (1b)$$

where $\tau = \tau_{\text{R}} E_0/E_{\text{inf}}$ is the creep characteristic time.

When the deformation in a viscous material cannot be considered small, a simple approach is to combine the standard linear solid expression for the relaxation modulus and the neo-Hookean equations relating stresses and strains. This standard neo-Hookean viscoelastic solid model has been previously utilized to describe the

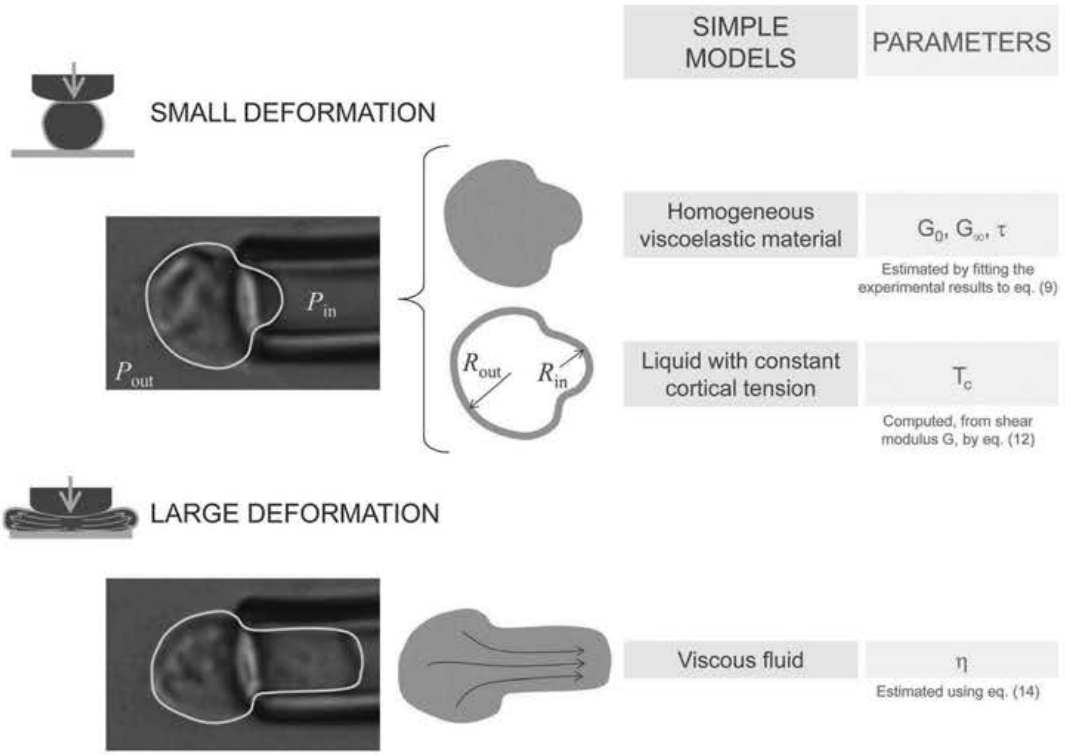

Fig. 1 Different simple approaches to describe the mechanical behavior of a cell. Cartoons of the three models considered in this work: homogeneous viscoelastic material model and liquid drop with constant cortical tension model for small deformation, and viscous fluid model for large deformation.

mechanical behavior of cells.[11,12] We used this model to characterize the cell behavior in the approximation of homogeneous viscoelastic solid and in the small, or relatively small, deformation regime (see Fig. 1).

Typically, cells in suspension have a spherical shape, which is explained by the cortical tension, in a similar manner to a suspended drop of liquid, where the shape is determined by the surface tension. Therefore, the second simple (above-mentioned) approach is to consider the cell as a liquid drop, of negligible viscosity, with the cortex under constant tension. In micropipette aspiration experiments, the cortical tension is easily determined from the spherical surfaces of the cell inside and outside the microcapillary.[1,14] In fact, *Dictyostelium* cells have been analyzed on some occasions using the liquid drop and cortical tension model.[15,17]

Actually the cytoplasm is neither an ideal liquid of negligible viscosity nor a homogeneous solid and, consequently, these two simple models, frequently used to interpret the mechanical tests of cells, are both approximations to a more complex reality. Below we analyze the relation between the parameters calculated for the two models.

The liquid drop and cortical tension model predicts that, in a micropipette aspiration experiment, when the length of suction surpasses the radius of the microcapillary the cell is unable to stay in equilibrium and it is freely aspirated. The results for cells with low viscosity are close to this description.[1,18] Other cells are much more viscous[24] and the flow of cytoplasm during the aspiration corresponds to a more viscous fluid. *Dictyostelium* cells are highly viscous, as we show in this work.

Linear equation for the viscoelastic cell

As explained above, we are firstly interested in the model of a homogeneous solid. In this case, the simplest analysis for the aspiration process is to approximate the cell by a half-space behaving as a linear elastic material.[25] The solution for the aspirated length is then

$$\frac{L_p}{R_p} = \frac{3\Phi_p \Delta P}{2\pi E} = C_{hs}\frac{\Delta P}{G}, \qquad (2)$$

where L_p is the aspirated length (see Fig. 2), R_p is the radius of the micropipette, ΔP is the differential pressure (pressure outside minus pressure inside the microcapillary), E is the Young's modulus and G is the shear modulus, or alternatively $1/G$ is the shear compliance. Φ_p is a pipette geometric factor that depends on the ratio between the thickness of the micropipette wall and its internal radius. It can be taken as approximately 2.1 for the punch model when the wall of the micropipette is relatively thick, as is the case in the aspiration experiments.[25] For an incompressible material $E = 3G$, and the constant C_{hs} is equal to 0.334. Usually the cells are considered approximately incompressible during the deformation. In agreement with this hypothesis, we found in this work that the computed volume of *Dyctiostelium* cells remained nearly constant during the aspiration process, within the experimental error (see Experimental section).

The disadvantage of the linear solution for the half-space model is that it does not take into account the finite size of the cells. Therefore such a solution is a reasonable approximation

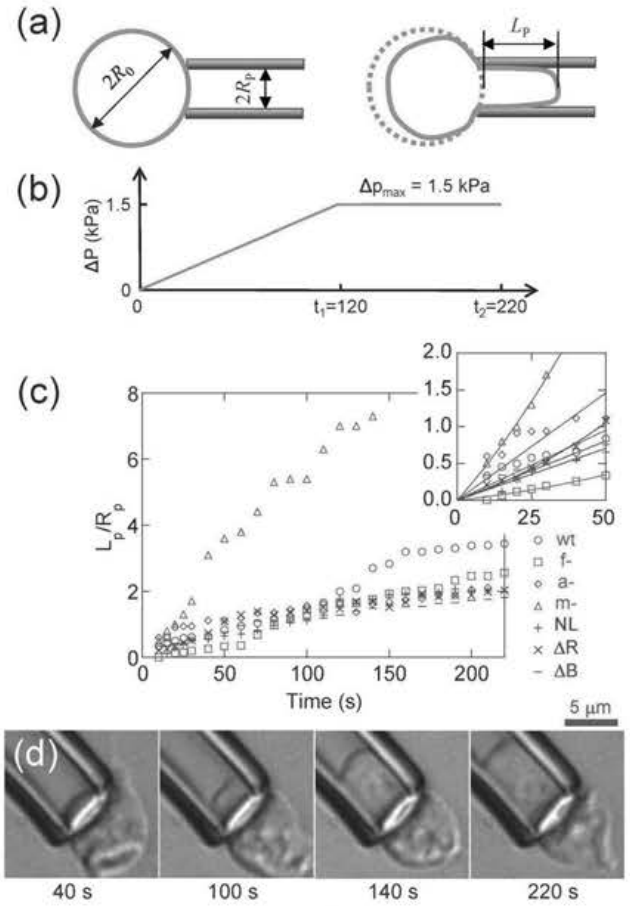

Fig. 2 Description of the experiments. (a) Sketch showing the definitions of initial radius of the cell R_0, internal radius of the micropipette R_p and aspirated length L_p. (b) Evolution of the applied differential pressure as a function of time. (c) Example curves L_p/R_p *vs.* time for the different cell lines studied: wild type AX-2 (wt), filamin-null (f-), α-actinin-null (a-) and myosin-null (m-) cells, and mutants expressing wild type myosin with normal neck length, (NL), ΔRLCBS myosin (D*R*) and ΔBLCBS myosin (D*B*); in these experiments, cells with $R_p/R_c \approx 0.6$ were selected, so that the differences were not affected by the size; and the fitted curves obtained using eqn (9) for the initial part of the experimental curves are also shown (see Appendix). (d) Images of the wild type AX-2 cell at different times during the experiment shown in (c).

only for very large cells and it introduces significant errors when the cells are not large. To analyze the effect of the size of the cells, Zhou *et al.*[11] studied numerically the deformation of a spherical cell, using a neo-Hookean model for the material. By fitting their solutions for different sizes of cells and different pressure differences, they obtained an equation for the dimensionless differential pressure $\Delta P/G$ as a function of L_p/R_p and R_p/R_0, which can be written as

$$\frac{L_p}{R_p} = C_s\left(\frac{L_p}{R_p}, \frac{R_p}{R_0}\right)\frac{\Delta P}{G}, \tag{3}$$

where R_0 is the initial radius of the cell. The equation was obtained for $0.25 \leq R_p/R_c \leq 0.6$ and $0 \leq \Delta P/G \leq 2.5$. The dimensionless function C_s depends on the two dimensionless parameters L_p/R_p and R_p/R_c. For example, $C_s(0.1,0.25) = 0.48$ and $C_s(0.1,0.6) = 0.70$, significantly higher than the constant C_{hs} obtained for the half-space model. The aspirated length L_p is proportional to the shear compliance $1/G$.

Li *et al.*[26] obtained an equation for L_p assuming linear elasticity and in which both the elastic modulus and the Poisson's ratio are parameters. This expression would be appropriate for the studies where incompressibility is not verified and for linear elasticity, though the effects of Poisson's ratio and elastic modulus cannot be separated for a given cell size. In our experiments, the cells were aspirated with – taking into account the experimental error (see Experimental section) – no significant changes in volume.

For the sake of simplicity and to facilitate additional analysis (see below), we aimed to approximate the previous equation by a linear one. We obtained such a linear approximation assuming small values of the aspirated length, thus using a Taylor series and retaining only the first power of the ratio L_p/R_p. The result is the following linear relation between dimensionless aspirated length and dimensionless differential pressure:

$$\frac{L_p}{R_p} = C_1\left(\frac{R_p}{R_0}\right)\frac{\Delta P}{G}, \tag{4}$$

where the function $C_1(R_p/R_c)$ takes into account the relative size of the cell and is given by

$$C_1\left(\frac{R_p}{R_0}\right) = \frac{1}{\beta_1\left[1 - \left(R_p/R_0\right)^{\beta_3}\right]}, \tag{5}$$

where $\beta_1 = 2.0142$ and $\beta_3 = 2.1187$ are constants obtained by Zhou *et al.* The difference between C_1 and C_s is less than 8% for $L_p/R_p \leq 0.1$ and $R_p/R_0 \geq 0.4$ (the latter condition is true in all our experiments). Recapitulating, eqn (2), corresponding to aspirating a linear-elastic half-space, is now corrected with the factor given by eqn (5) to take into account the finite size of the cells.

The time-dependent response of viscoelastic materials is usually described by a three-parameter viscoelastic model, *i.e.* standard linear solid. Consistent with eqn (1b), the shear creep compliance may be written as

$$\frac{1 - \alpha_1 e^{-t/\tau}}{G_0(1 - \alpha_1)}, \tag{6}$$

where G_0 is the initial shear modulus (for time $t = 0$), α_1 is a dimensionless coefficient, $G_{inf} = G_0(1 - \alpha_1)$ is the shear modulus for infinite time and τ is the creep characteristic time, related to the relaxation time τ_R by $\tau = \tau_R G_0/G_{inf}$. This equation is equivalent to eqn (1). The linear-viscoelastic solution for half-space geometry and small deformation, when the differential pressure is applied instantaneously at $t = 0$, is obtained by replacing the shear compliance in eqn (2) by the creep shear compliance[4,12,25,27]

$$\frac{L_p(t)}{R_p} = C_{hs}\frac{\Delta P}{G_0}\frac{1 - \alpha_1 e^{-t/\tau}}{1 - \alpha_1}. \tag{7}$$

As a linear approximation for small deformation, taking into account the finite size of the cell, we used this equation corrected by the factor in eqn (5), *i.e.*

$$\frac{L_p(t)}{R_p} = C_1\left(\frac{R_p}{R_0}\right)\frac{\Delta P}{G_0}\frac{1 - \alpha_1 e^{-t/\tau}}{1 - \alpha_1}. \tag{8}$$

In the tests, we applied a constant rate $d\Delta P/dt = 12.5$ Pa s^{-1} during the first 120 s (see Fig. 2). For this stage, the equation governing the process is obtained from Boltzmann's superposition principle:

$$\begin{aligned}\frac{L_p(t)}{R_p} &= \int_0^t C_1\left(\frac{R_p}{R_0}\right)\frac{1-\alpha_1 e^{-\frac{t-s}{\tau}}}{G_0(1-\alpha_1)}\frac{d\Delta P}{dt}ds \\ &= C_1\left(\frac{R_p}{R_0}\right)\frac{t-\alpha_1\tau\left(1-e^{-t/\tau}\right)}{G_0(1-\alpha_1)}\frac{d\Delta P}{dt}\end{aligned} \tag{9}$$

To find the values of G_0, $G_{inf} = G_0(1-\alpha_1)$ and τ we fitted this equation to the initial part of the experimental curve aspirated length *vs.* time. To display the results, we decided to represent the elastic modulus E assuming incompressibility, *i.e.* $E_0 = 3G_0$ and $E_{inf} = 3G_{inf}$. See Appendix for more details on the use of eqn (9) to fit the experimental curves.

Cortical tension: relation between the measurements of viscoelastic parameters and the measured cortical tension

The equilibrium shape of a drop of liquid, when aspirated by a microcapillary, depends exclusively on the surface tension T. As shown in Fig. 1, the equilibrium shape corresponds to spherical surfaces inside and outside the microcapillary, respectively with radii R_{in} and R_{out}. The relation between curvatures, surface tension and differential pressure is given by the Laplace equation:

$$\Delta P = 2T\left(\frac{1}{R_{in}} - \frac{1}{R_{out}}\right) \tag{10}$$

For the cell, considering that the cortex thickness is small, the cortical tension T_c takes the place of the surface tension in eqn (10). It is possible to calculate the equivalence between the estimations of cortical tension given by eqn (10) and of shear modulus given by eqn (4). To obtain such a relation, we observed that the initial radius of the cell R_0 and the radius of the inner spherical surface are related by $L_p + R_0 - (R_0^2 - R_p^2)^{1/2} = R_i - (R_i^2 - R_p^2)^{1/2}$, and thus $dL_p = [1 - R_i(R_i^2 - R_p^2)^{-1/2}]dR_i$. Besides, $d(1/R_i) = -dR_i/R_i^2$ and for small deformation $1/R_{in} - 1/R_{out} \approx 1/R_{in} - 1/R_0$. Finally, combining these equations for the small deformation limit (small value of L_p), we can write

$$\frac{1}{R_{in}} - \frac{1}{R_{out}} \approx \frac{R_p}{R_0^2\left[\left(1-\left(R_p/R_0\right)^2\right)^{-1/2} - 1\right]}\frac{L_p}{R_p}. \tag{11}$$

And, combining eqn (4), (10) and (11),

$$T_c = \frac{R_0^2\left[\left(1-\left(R_p/R_0\right)^2\right)^{-1/2} - 1\right]}{2R_pC_1\left(\frac{R_p}{R_0}\right)}G. \tag{12}$$

In the calculations we estimated the extreme values of the shear modulus, *i.e.* the initial value G_0 and the value for infinite time G_{inf}, and computed the apparent cortical tension for both times using eqn (12). Therefore the value obtained in this way should coincide with the value measured in other works.

Overall viscosity of the cells

When a cell undergoes large deformations, it evolves from a solid-like to a fluid-like state.[5,28] In fact, when the whole cell is aspirated by a micropipette, the liquid-like cellular material flows into the microcapillary and it is possible to quantify the apparent viscosity,[18,19] which has been done most frequently for relatively low-viscosity cells like neutrophils.[18,21,29]

Following the result by Needham and Hochmuth[18] and as described in a previous study,[30] it is possible to estimate the overall viscosity of the cells by measuring the fraction of volume aspirated inside the microcapillary, at constant pressure, for a given time. In our experiments the pressure increases at constant rate from the initial time $t = 0$ to the time $t_1 = 120$ s, and then the differential pressure $\Delta P_{max} = 1.5$ kPa is maintained constant up to the final time $t_2 = 220$ s. The ratio between aspirated volume V_{in} (at t_2) and the total volume of the cell V_{tot} is given by

$$\begin{aligned}\frac{V_{in}}{V_{tot}} &= \frac{3}{4m\mu\left(1-R_p/R_0\right)}\left(\frac{R_p}{R_0}\right)^3\int_0^{t_2}\Delta P\,dt \\ &= \frac{3\Delta P_{max}(t_2 - t_1/2)}{4m\mu\left(1-R_p/R_0\right)}\left(\frac{R_p}{R_0}\right)^3,\end{aligned} \tag{13}$$

where R_0 is the initial radius of the cell, m is a constant with a value $m = 6$ and μ is the apparent viscosity of the cell. The approximation was found to be valid in the range $R_0/R_p < 2.5$ and $V_{in}/V_{tot} < 0.45$.[30] From eqn (13), the apparent viscosity is given by

$$\mu = \frac{3\Delta P_{max}(t_2 - t_1/2)}{4m\frac{V_{in}}{V_{tot}}\left(1-\frac{R_p}{R_0}\right)}\left(\frac{R_p}{R_0}\right)^3. \tag{14}$$

Therefore, for a given cell, the apparent viscosity is calculated using eqn (14), and quantifying the aspirated volume V_{in}, the total volume V_{tot} and the initial radius of the cell R_0 (*i.e.* the radius of a sphere of volume V_{tot}) from the microscopy image at time t_2. The details for the analysis of the experimental results to compute the apparent viscosity may be found in the previous work by Plaza *et al.*[30]

Experimental results

To study the effect of ABPs on the deformability of the cells, we analyzed firstly the consequence of the absence of one of the three proteins considered: α-actinin and filamin, which act as passive cross-linkers of the actin filaments, and non-muscle myosin II (for simplicity we use the name myosin throughout the text), which works as a molecular motor to drive the contractile behavior of the cytoskeleton and acts as an active cross-linker. Secondly, we studied the behavior of mutant cells expressing myosins with different lengths of the neck region:[31] wild type myosin (normal length, 8.8 nm), ΔRLCBS myosin (5.8 nm) and ΔBLCBS myosin (1.8 nm). This region acts as a lever arm to displace the myosin motor relative to the actin filaments.[32]

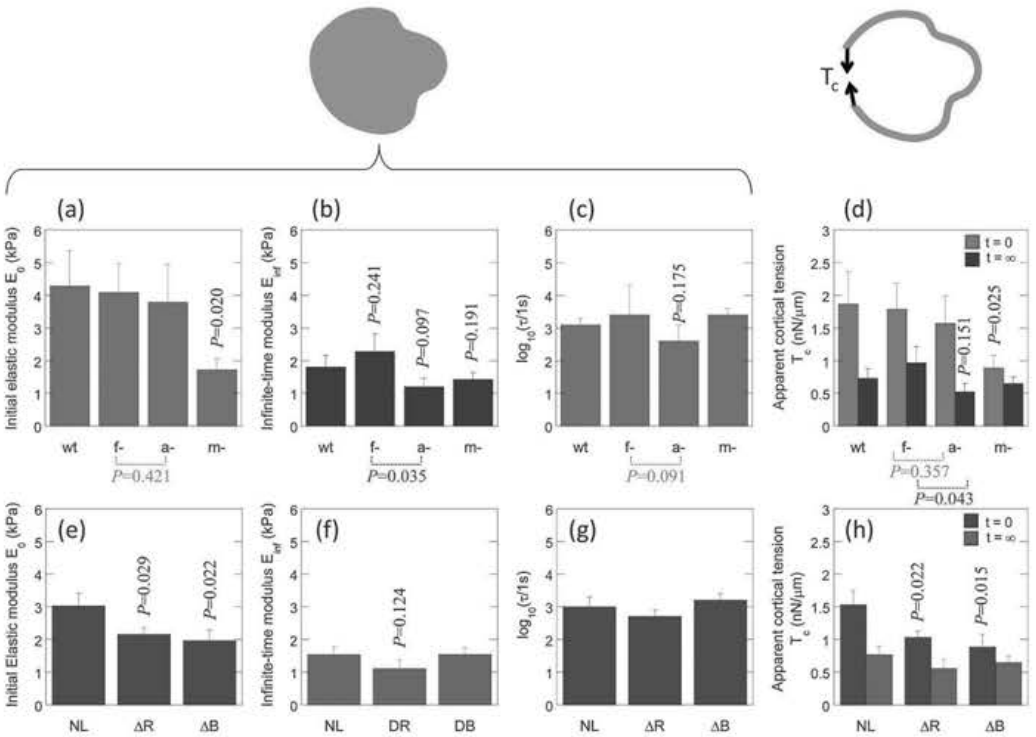

Fig. 3 Mechanical parameters obtained for small deformation: initial elastic modulus E_0 (a, e), infinite time elastic modulus E_{inf} (b, f), creep characteristic time τ (c, g) and cortical tension T_c (d, h). Graphs a–d show the results for wild type AX-2 (wt, N = 25 cells), filamin-null (f-, N = 16), α-actinin-null (a-, N = 15) and myosin-null (m-, N = 20) cells. Graphs e–h show the results for mutants expressing wild type myosin with normal neck length (NL, N = 27), ΔRLCBS myosin (ΔR, N = 19) and ΔBLCBS myosin (ΔB, N = 24). The P-value is indicated with respect to the reference cell: wt in graphs a–d and NL in graphs e–h. P-values for the difference between filamin-null and α-actinin-null cells are also included. Error bars represent standard errors.

Fig. 3 shows the estimated values for the viscoelastic parameters (homogeneous viscoelastic model) and the apparent cortical tension (liquid drop and cortex model) obtained by fitting the experimental data (see Fig. 2b). For the sake of familiarity, we chose to represent the elastic modulus E instead of the shear modulus G. Under the assumption of incompressibility, $E = 3G$. To quantify the accuracy of the fittings in the small deformation regime, we computed the mean squared relative error, MSRE, for each experiment. The average MSRE value for each type of cell was 0.24 (wilt type AX-2 cells), 0.22 (filamin-null), 0.24 (α-actinin-null), 0.20 (myosin-null); 0.21 (mutants expressing wild type myosin), 0.12 (ΔRLCBS myosin) and 0.29 (ΔBLCBS myosin).

It can be observed in Fig. 3a that, for short times, the absence of myosin II results in a significantly more compliant behavior, being the initial elastic modulus E_0 1.7 ± 0.3 kPa for myosin-null cells and 4.3 ± 1.0 kPa for wild type cells. For long times, however, filamin-null cells do not show a more compliant behavior and α-actinin-null cells show the lowest value of the elastic modulus for infinite time, E_{inf} (Fig. 3b). This parameter ranges between 1.4 ± 0.2 kPa for α-actinin-null cells and 2.3 ± 0.5 kPa for filamin-null cells.

In the case of the mutants expressing different myosin molecules, Fig. 3e shows that E_0 is lower for myosins with shorter neck regions: from 3.0 ± 0.4 kPa for normal-length myosin to 2.0 ± 0.3 kPa for ΔBLCBS myosin. E_{inf} is similar for the three types, around 1.4 kPa, with less significant differences.

Regarding the creep characteristic time τ, we obtained a large dispersion of results over several orders of magnitude and therefore we considered it convenient to analyze the logarithmic value. The mean values are of the order of 10^2–10^3 s for all the cell lines, with relatively low differences, the lowest value being for α-actinin-null cells, with a mean value of $10^{2.6} \approx 400$ s (*vs.* ≈1300 s for wt cells).

For the liquid drop and cortex model, the only parameter is the cortical tension T_c, and the results are shown in Fig. 3d and h. As explained previously, we estimated T_c with eqn (12), using G_0 or G_{inf} to compute the cortical tension that would be measured respectively at a short time or a long time after the application of the differential pressure. Consequently, the values of the cortical tension follow the same trend as the values of the elastic modulus.

Fig. 4 shows the results for the measurements of the volume of the cell aspirated during the whole duration of the experiments, 220 s, and the resulting estimated values of the apparent viscosity (using one image in each experiment as described in the previous work by Plaza *et al.*[30]). As a general rule, the trend is the same as for the initial elastic modulus: the deformability is higher for the mutant cells lacking one ABP, as reflected in a higher aspirated volume during the test. Fig. 4a shows that overall the highest aspirated volume corresponds to myosin-null cells, followed by α-actinin-null cells and filamin-null cells. Fig. 4c shows that the differences for the cells expressing different myosins are relatively small though, on the whole, the

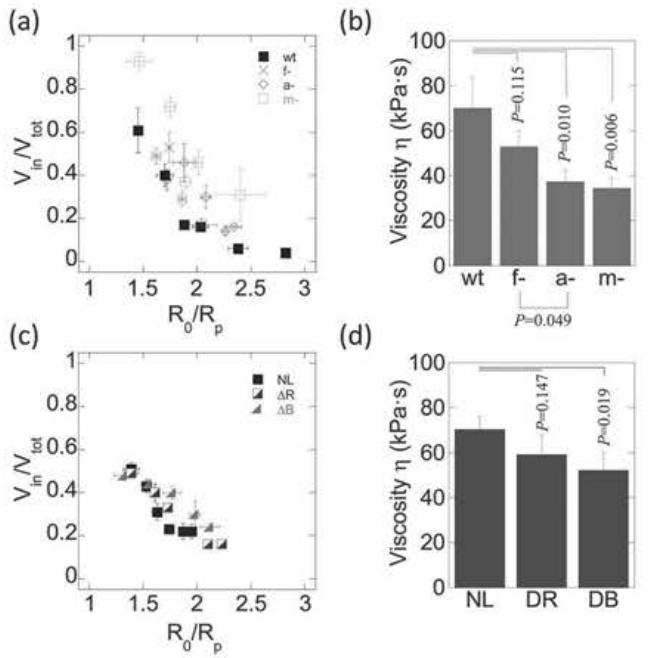

Fig. 4 Results for large deformation. (a, c) Relative aspirated volume (V_{in}, divided by total volume of the cell V_{tot}) *vs.* the initial radius of the cell (R_0, divided by the radius of the capillary R_p). (b, d) Estimated apparent viscosity.[30] The labels are the same as in Fig. 3. Error bars represent standard errors.

aspirated volume is lowest for wt myosin, the highest corresponding to ΔBLCBS myosin. The values for the estimated apparent viscosity are presented in Fig. 4b and d. The viscosity was calculated using eqn (14) within the admissible range of relative aspirated volume (V_{in}/V_{tot}), as explained above. For wild type (AX2) cells the viscosity is 70 ± 13 kPa s, similar to the mutant cells expressing wt myosin, 70 ± 13 kPa s. The viscosity is significantly lower for myosin-null cells (34 ± 5 kPa s) and α-actinin-null cells (37 ± 5 kPa s), while being intermediate for filamin-null cells (53 ± 7 kPa s). Cells with reduced-length myosins also show lower viscosity: 59 ± 9 and 52 ± 8 kPa s respectively for ΔRLCBS and ΔBLCBS, the latter one being significantly lower than the reference value for wt myosin.

Discussion

Use of the three models and comparison with previous work and other cell types

As explained in the Results section, the average MSRE values for the different cells are in the range 0.12–0.29. Apart from the experimental error, these values reflect the limits of considering the cells as passive, homogeneous, viscoelastic and spherical materials: in practice (see Fig. 2) the aspiration process occurs in a more irregular manner than the continuous advance predicted by eqn (9), which can be attributed in part to the inhomogeneity and the active changes in the living cells. The inhomogeneity of the cells also produces variability in the measured elastic modulus: higher if the aspirated region includes the nucleus and lower if the nucleus is in the opposite part of the cell. Even with these limitations, the parameters obtained by fitting are assumed to describe an averaged mechanical behavior of the cells.

The mechanical parameters calculated here are in agreement with previous works where the cortical tension of *Dictyostelium* cells was evaluated:[15,17] 1.1–1.5 nN μm^{-1} for wild type cells, 0.6–0.8 nN μm^{-1} for myosin II-null cells, ~0.95 nN μm^{-1} for filamin-null cells and ~0.8 nN μm^{-1} for α-actinin-null cells. Although there are some differences in the values reported, they are all in the range that we have obtained from zero to infinite time. Such differences may be explained by the fact that in those works the measurements were carried out neglecting the viscous component of the mechanical behavior of the cells. On the contrary, our characterization shows the importance of considering the time when analyzing the shape of the cell submitted to a constant differential pressure during aspiration with a micropipette. This reasoning justifies the idea that for a short time and small deformation the homogeneous elastic material would be the best simplistic approach to characterize the mechanical response of the cell, as both cytoskeleton and inner materials contribute to resist the forces and to the shape of the cell. For a long time, the viscous deformation of the inner materials would have concluded in the main and the equilibrium shape would be determined primarily by the cortical tension T_c. In the previous section we have estimated that the creep characteristic time is of the order of minutes or tens of minutes for *Dictyostelium* cells. Finally, for large deformation, the apparent viscosity describes conveniently the viscous flow of the cellular materials.

The three simplistic models do not take into account other possible, additional, inhomogeneities. For instance Luo *et al.*[17] perceived by fluorescence microscopy an increased concentration of ABPs on the aspirated region of the cell, which could contribute to stiffening that particular region, thus contributing to a higher stiffness, as measured by micropipette aspiration.

The elastic modulus obtained for *Dictyostelium* cells indicates that these are relatively stiff cells, similar to some types of mammalian cells, including fibroblasts, muscle cells, osteoblasts and chondrocytes, whose elastic modulus may be of the order of a few kPa.[33,34] Differently, adipocytes and white blood cells are typically one or two orders of magnitude more compliant.[30,33,35]

Dictyostelium cells also appear as highly viscous. Viscosities of the same order of magnitude have been reported for chick embryo fibroblasts, at 20–40 kPa s.[24] In these cells the cytoskeleton is an important component and they are able to form actin stress fibers. Contrarily, neutrophils were found to behave as a much less viscous fluid, with an apparent viscosity in the range of 0.06–0.5 kPa s.[18,21,29] This lower viscosity should play an important role regarding the ability of neutrophils to pass through capillaries and migrate into tissues.

Influence of the actin-binding proteins

The three ABPs studied here provide cross-links for the network of actin filaments. In addition, myosin filaments act as molecular motors, driving the contractile behavior of the cytoskeleton – by producing the approaching of actin filaments bound to the

myosin heads in both extremes of myosin filaments – and actively introducing cortical tension. The results show that, as one would expect, the absence of myosin or α-actinin results in a higher deformability (the influence of filamin is lower, with no significant differences), whether analyzing the large deformations through the apparent viscosity, or using the model of homogeneous solid or considering the cortical tension. In this last case, the same trend was found in other studies.[15,17] Moreover, the deformability also increases if the myosin molecules are replaced by recombinant myosins with reduced neck length, and the same trend is found in the three different mechanical models considered. Reasonably, the relation of deformability to myosin characteristics is compatible with the idea that the main contribution of myosin molecules to stiffening the cells during the deformation process is to resist the molecular forces as a cross-linking molecule, surpassing the effect of dynamically introducing a contractile stress.

The ability of myosin II to resist forces while attached to actin filaments has been explained in terms of the effective detachment rate constant, k_{off}, using the Arrhenius transition state theory.[36] The rate constant is assumed to be dependent on the force F applied to the head (Fig. 5a): $k_{off} = k^0_{off} \exp(-F\Delta x/k_B T)$, where k^0_{off} is the rate constant in the absence of force and Δx is the displacement of the molecule – by rotation of the neck region – in the direction of the force (thus $F\Delta x$ is the work exerted by the molecule against the pulling force). It was confirmed experimentally that the detachment rate decreases exponentially with the applied force.[36,37] For the different myosins, the longer the length of the neck, the longer the distance Δx as the myosin neck rotates. Therefore, the mutant cells expressing wt myosin, *i.e.* the cells with the longest Δx, are expected to be the most sensitive to pulling forces (Fig. 5a),[31] and this would provide an explanation for the higher stiffness and viscosity of these cells. In this regard, it has been found that the contraction

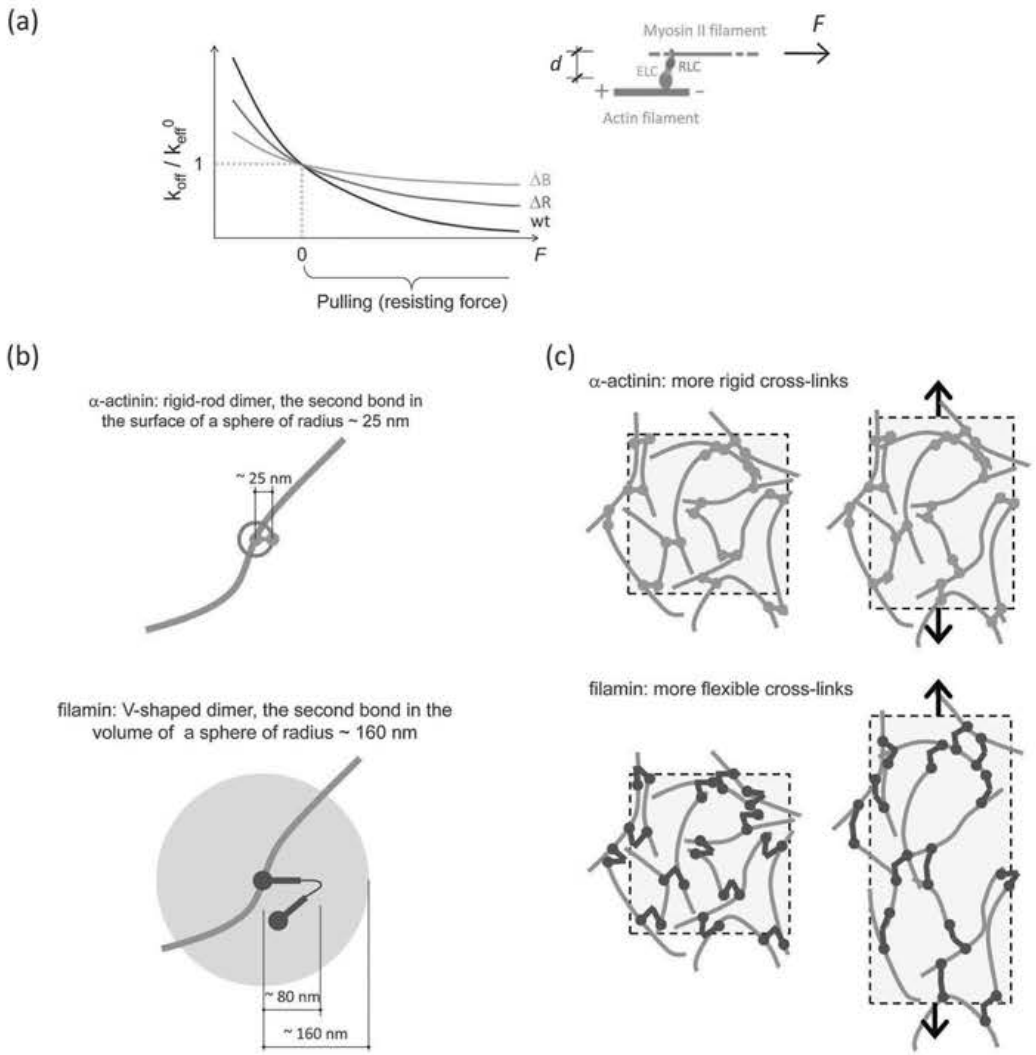

Fig. 5 Schematic description of the behavior of the studied ABPs. (a) The detaching rate of myosin heads from actin filaments decreases as the opposing force increases.[36] (b and c) Proposed comparison between filamin and α-actinin: (b) the different structure and size determine the higher rigidity and limitation to establish cross-links of α-actinin (in the sketch we ignore the fact that the second bond could not be established in all directions); (c) the higher flexibility of filamin cross-links results in a larger deformability of the network.[39]

speed of cytoskeletons is more affected by external forces for wt myosin than for ΔRLCBS and ΔBLCBS myosins.[38]

The effects of filamin and α-actinin on the deformability are different: the absence of α-actinin results in a lower viscosity of the cell, while the effect of the absence of filamin is lower (no significant differences). Furthermore, α-actinin-null cells show the lowest characteristic time τ (the difference between both cell lines yields a *P*-value of 0.091, *i.e.* marginally significant) and the lowest elastic modulus E_{inf} (the difference between both cell lines is significant, *P*-value = 0.035, the difference between wt cells and acninin α-null cells is marginally significant, *P*-value = 0.097) or alternatively the lowest cortical tension for long times $T_c(t = \infty)$ (*P*-value = 0.043), suggesting that replacing α-actinin cross-links by filamin cross-links results in a higher deformability of the cortex. Therefore, our results indicate that α-actinin contributes especially to impeding the deformation of the cells. In a previous work, we studied the myosin-driven contraction of *Dictyostelium* actomyosin cytoskeletons – of cells after removing the plasma membrane – and found that the cytoskeletons are much more easily deformable and contract faster in the absence of α-actinin, and they disintegrate during the contraction in the absence of filamin.[38]

The different cross-linking possibilities of filamin and α-actinin have been analyzed previously in terms of their different structures:[17,40,41] the V-shaped filamin dimer with 160 nm (2 × 80 nm) of extended length[42] and the rod-shaped antiparallel α-actinin dimer with a length of 24 nm.[43,44] In this sense, by observing the accumulation of proteins in the cortex during micropipette aspiration of *Dictyostelium* cells deficient in different proteins and using numerical models, Luo *et al.* proposed that filamin, assumed to connect preferably non-parallel filaments, could be more sensitive to shear deformation, while α-actinin, presumed to link preferably parallel filaments, could be more sensitive to dilation deformation.[17] In a different study, Courson *et al.* reported that α-actinin links actin filaments over all angles of filament orientation,[20] and other studies showed the ability of both α-actinin and filamin to link filaments in similar orientations and resist forces of comparable values when single filaments are pulled.[45]

Reaction rates and single molecule studies provide useful information to interpret the different behavior, and some previous studies measured the properties of filamin and α-actinin, though using different species so that the numerical values could be different for *Dictyostelium* homologues. In this regard, a previous study by Goldmann *et al.* on the association of filamin and α-actinin to filamentous actin found values of the overall association rate constant, k_{on}, 30% higher for filamin, and of the overall dissociation rate constant, k_{off}, 50% higher for filamin (≈ 0.6 *vs.* ≈ 0.4 s^{-1}).[46] Although that study did not take into account the whole complexity of the cytoskeleton nor the dynamic deformation process, the higher rate constants for filamin point to an easier remodeling of cytoskeleton with filamin and without α-actinin compared to a cytoskeleton with α-actinin and lacking filamin. Ferrer *et al.* measured the molecular rupture forces between single actin filaments and ABPs, also finding a higher dissociation rate for filamin (0.087 ± 0.073 *vs.* 0.066 ± 0.028 s^{-1}) compared with α-actinin and a slightly different dependency on the loading rate,[45] with the limitation that in these experiments the actin filaments were loaded with directional force. An intermediate value of $k_{off} \approx 0.05$ s^{-1} for α-actinin was measured with an optical trap technique.[47]

The different intrinsic flexibility and size of both ABPs are also important characteristics (see Fig. 5b and c): while the α-actinin dimer is rigid and shorter, the filamin V-shaped dimer is more flexible and can be extended from a small to a large angle. The largest angles may correspond to a relatively high energy and therefore the largest extension may require the application of an external load.[48] The consequences of these differences are important: firstly, for small deformation, the higher stiffness of α-actinin compared to filamin results in a reasonably more stiff cytoskeletal network if the cross-links are provided by α-actinin than if the cross-linking protein is filamin. Therefore, the relative content of filamin and α-actinin modulates the deformability of the material. Consequently, assuming an equivalent concentration of cross-links in the cortex, the tendency expected for small deformation is a higher stiffness for filamin-null cells when compared to α-actinin-null cells (Fig. 5b). Secondly, the longer length of filamin and its higher flexibility could allow it to establish cross-links between relatively distant actin filaments, while the short length and rigidity of α-actinin limits the possibility of establishing cross-links to nearby filaments (Fig. 5c). These differences provide an explanation for the different behavior of contracting cytoskeletons: on the one hand, the longer lifetime of α-actinin cross-links obstructs the remodeling of the network and results in a higher elastic modulus; on the other hand, the lower ability of α-actinin to establish new cross-links (due to the lower rate constant, lower flexibility and shorter length) would facilitate the disintegration of cytoskeletons in the absence of filamin and the plasma membrane, as described in our previous work.[38]

The main experimental results and the related molecular mechanisms discussed above are shown in Table 1. To summarize, our results confer new experimental evidence for the already described effect of myosin and the proposed molecular mechanisms, we provide new mechanical results for the influence of filamin and α-actinin and we propose the molecular mechanisms explaining their different effects, based on previous studies of these molecules. The analytical methodology described in this work allows differentiation of the effect of the two cross-linking proteins in the different regimes of deformation.

The different deformability and contractile speed related to the ABPs suggests a mechanism for the cell to adapt its behavior to the ambient conditions by modifying the relative content of filamin and α-actinin. In fact, filamin has been identified as a signaling center for various proteins. It has been found that this molecule acts as a force-sensor[49,50] and the mechanism would be the effect of stretching the molecule on the affinity between the target peptides and the binding sites in the filamin molecule. This idea is supported by studies of mechanically strained filamin cross-linked actin networks[41] and single-molecule experiments.[48]

Table 1 Experimental results obtained by micropipette aspiration in the present work, and by studying the contraction of cytoskeletons in the previous work by the authors,[38] and the proposed related molecular mechanisms, as explained in the discussion section

		Myosin	Filamin	α-actinin
Observed	Aspiration experiments (present work)	for shorter lever arm: • lower rigidity (E_0, P=0.029 ΔR, P=0.022 ΔB) • lower cortical tension ($T_c(0)$, P=0.022 ΔR, P=0.015 ΔB) • lower viscosity (P=0.019 ΔB)	• low influence (not significant differences)	in the absence of α-actinin: • lower viscosity (P=0.010) • moderately lower rigidity (E_{ref} marginally significant, P=0.097, significant vs. f- cells, P=0.035) • moderately lower characteristic time (marginally significant vs. f- cells, P=0.091)
	Cytoskeletal contraction (in the previous work[38])	• lower contraction speed for shorter lever arm	• disassembly of the cytoskeletons in the absence of filamin	• in the absence of α-actinin, significant increase of contraction speed and deformability
				
Molecular mechanisms		• lifetime of the myosin-actin bond increases with resistive force F • for no resistive force F, larger lever arm provides higher sliding speed	lower molecular stiffness and higher dissociation rate constant: • low contribution to stiffness • it maintains connectivity of the network, allowing remodelling	higher molecular stiffness and low rate constants: • it strongly impedes deformation

Experimental

Cell lines

The source of the cells used in this work was described in a previous article.[38] Briefly, the wild type (wt) *Dictyostelium discoideum* cells correspond to the AX2 strain, an axenically growing strain. To study the influence of ABPs, we used mutant *D. discoideum* strains lacking α-actinin or filamin generated and described in previous studies.[51,52] These strains were obtained from the Dicty Stock Center, and their strain IDs were DBS0235459 and DBS0236077, respectively. AX2 is the parent strain of these two mutants, and was tested as the wt reference. The cells were maintained on plastic Petri dishes in HL5 medium[53] containing an additional 60 μg each of penicillin and streptomycin per mL (thus named HL5PS) at 24 °C. We used also the mutant *Dictyostelium discoideum* cell line HS1[54] that lacks the unique myosin II heavy chain gene.

To study the influence of the characteristics of the myosin molecules, HS1 cells were transfected with pTIKL (extrachromosomal vector with a G418-resistance gene) carrying each one of the mutant or wt myosin II heavy chain genes that were fused N-terminally with the S65T mutant GFP gene. Transfected cells were selected and maintained in HL5PS medium in the presence of 12 μg mL^{-1} G418 (Invitrogen, Tokyo, Japan). The three different types of myosin II heavy chain are: (a) wild type (NL), (b) mutant myosin with an internal deletion that removes the regulatory light chain binding site, ΔRLCBS,[55] and (c) a mutant lacking both light chain binding sites, ΔBLCBS.[31]

Micropipette aspiration tests and digital analysis

The micropipette aspiration tests were conducted at 24 °C following the procedures described previously.[9,12] Before starting the experiments, the cells were resuspended and then tested in culture medium. The internal diameter of the micropipette was approximately 5 μm.

The number of tested and analyzed cells is included in the caption of Fig. 3 and was, for each type: 25 wt, 16 filamin-null, 15 α-actinin-null, 20 myosin-null, 27 mutant-expressing wt myosin, 19 mutant-expressing ΔRLCBS myosin and 24 mutant-expressing ΔBLCBS myosin cells.

The aspiration process was studied by time-lapse imaging and using phase contrast microscopy. Each experiment was examined to obtain the parameters corresponding to the three material models used in this work. The images were analyzed with the software ImageJ (http://rsb.info.nih.gov/ij), to measure the aspirated length L_p of cellular material inside the microcapillary. To quantify the volumes in the final situation, the volume inside the microcapillary was approximated by a cylinder and a hemisphere and the volume outside the microcapillary was approximated by an ellipsoid. The aspirated volume (V_{in}) was calculated as the volume inside the microcapillary minus the spherical cap, corresponding to the initial volume of the cell inside the microcapillary. Curve fittings were carried out using the Levenberg–Marquardt algorithm and the software Kaleidagraph (Synergy Software, Reading, PA, USA). Fittings, as explained in the Appendix, were performed for the first part of the experimental curves, including at least five experimental points. In our pictures, the internal diameter of the micropipette was approximately equal to the length of 50 pixels and assuming that the error of length measurement is of the order of 1 pixel (4% of the internal radius R_p), our error in the non-dimensional length L_p/R_p is nearly 0.04. Moreover, for the calculations of viscosity, the aspirated volume is larger than R_p^3 and therefore the measurement error for this derived variable is lower than 12%.

Conclusions

We have developed a simple methodology, which easily takes into account the size of the cell, to quantify basic cell mechanical parameters from micropipette aspiration experiments.

The ABPs affect the deformability of the cell differently and we were able to relate the molecular characteristics and the mechanical response of the cell. For myosin, its effect is explained in terms of the relation between the lifetime of the bond to actin and the resistive force. Our analyses allowed differentiation of the effects of the two cross-linking proteins in the different regimes of deformation: the picture that arises is that the presence of α-actinin more intensely obstructs the deformation of the cytoskeleton (as shown by the mechanical results of the present work), presumably mainly due to the higher stiffness and to the lower rate constants, and that filamin contributes critically to the global connectivity of the network, possibly providing a rapid turn over of the cross-links during the remodeling of the cytoskeletal network, thanks to the higher rate constants, flexibility and larger size. This description also explains the lower characteristic time in α-actinin-null cells: the higher characteristic times in the other cell types would be related to the lower rate constants (*i.e.* higher bond lifetime) of α-actinin.

By regulating the expression levels of filamin and α-actinin, the cell might tune its own deformability, the contraction speed of the cytoskeleton and the mechanosensitivity associated to filamin.

Appendix

The fitting of the experimental curves using eqn (9) may be carried out rewriting the equation as follows:

$$\frac{L_p(t)}{R_p C_1 \left(\frac{R_p}{R_c}\right)\frac{d\Delta P}{dt}} = \frac{1}{G_0(1-\alpha_1)}t - \frac{\alpha_1 \tau}{G_0(1-\alpha_1)}\left(1 - e^{-t/\tau}\right). \quad (15)$$

Defining $y(t) = L_p(t) \Big/ \left[R_p C_1 \left(\frac{R_p}{R_c}\right)\frac{d\Delta P}{dt}\right]$, the experimental data (see Fig. 2b) are therefore fitted by the function

$$y(t) = At - B(1 - e^{-t/\tau}). \quad (16)$$

Thus one of the three viscoelastic parameters, τ, is obtained directly in the fitting and the other two may be computed as

$$\alpha_1 = \frac{B}{A\tau}; \quad G_0 = \frac{1}{A(1-\alpha_1)}. \quad (17)$$

For each fitting we computed the mean squared relative error, MSRE, as

$$\mathrm{MSRE} = \sum_{i=1}^{n} \left(\frac{y_{meas}(t_i) - y(t_i)}{y(t_i)}\right)^2, \quad (18)$$

with $y_{meas}(t_i)$ and $y(t_i)$ being respectively the measured value and the calculated value using the fitted parameters, at time t_i, and n the number of measurements.

The details for the analysis of the experimental results to compute the apparent viscosity may be found in the previous work by Plaza *et al.*[30]

Acknowledgements

The authors would like to thank Dr Krista Sider for her help during micropipette aspiration experiments.

References

R. M. Hochmuth, *J. Biomech.*, 2000, **33**, 15–22, DOI: 10.1016/S0021-9290(99)00175-X.

G. Bao and S. Suresh, *Nat. Mater.*, 2003, **2**, 715–725, DOI: 10.1038/nmat1001.

C. T. Lim, E. H. Zhou and S. T. Quek, *J. Biomech.*, 2006, **39**, 195–216, DOI: 10.1016/j.jbiomech.2004.12.008.

F. Guilak, J. R. Tedrow and R. Burgkart, *Biochem. Biophys. Res. Commun.*, 2000, **269**, 781–786, DOI: 10.1006/bbrc.2000.2360.

X. Trepat, L. Deng, S. S. An, D. Navajas, D. J. Tschumperlin, W. T. Gerthoffer, J. P. Butler and J. J. Fredberg, *Nature*, 2007, **447**, 592–595, DOI: 10.1038/nature05824.

M. P. Stewart, J. Helenius, Y. Toyoda, S. P. Ramanathan, D. J. Muller and A. A. Hyman, *Nature*, 2011, **469**, 226–230, DOI: 10.1038/nature09642.

P. Bursac, G. Lenormand, B. Fabry, M. Oliver, D. A. Weitz, V. Viasnoff, J. P. Butler and J. J. Fredberg, *Nat. Mater.*, 2005, **4**, 557–561, DOI: 10.1038/nmat1404.

W. R. Jones, H. P. Ting-Beall, G. M. Lee, S. S. Kelley, R. M. Hochmuth and F. Guilak, *J. Biomech.*, 1999, **32**, 119–127, DOI: 10.1016/S0021-9290(98)00166-3.

W. R. Trickey, G. M. Lee and F. Guilak, *J. Orthop. Res.*, 2000, **18**, 891–898, DOI: 10.1002/jor.1100180607.

F. Guilak, G. R. Erickson and H. P. Ting-Beall, *Biophys. J.*, 2002, **82**, 720–727.

E. H. Zhou, C. T. Lim and S. T. Quek, *Mech. Adv. Mater. Struct.*, 2005, **12**, 501–512, DOI: 10.1080/15376490500259335.

R. Zhao, K. Wyss and C. A. Simmons, *J. Biomech.*, 2009, **42**, 2768–2773, DOI: 10.1016/j.jbiomech.2009.07.035.

K. Wyss, C. Y. Y. Yip, Z. Mirzaei, X. Jin, J. Chen and C. A. Simmons, *J. Biomech.*, 2012, **45**, 882–887, DOI: 10.1016/j.jbiomech.2011.11.030.

D. V. Zhelev, D. Needham and R. M. Hochmuth, *Biophys. J.*, 1994, **67**, 696–705.

J. W. Dai, H. P. Ting-Beall, R. M. Hochmuth, M. P. Sheetz and M. A. Titus, *Biophys. J.*, 1999, **77**, 1168–1176.

R. Merkel, R. Simson, D. A. Simson, M. Hohenadl, A. Boulbitch, E. Wallraff and E. Sackmann, *Biophys. J.*, 2000, **79**, 707–719.

T. Luo, K. Mohan, P. A. Iglesias and D. N. Robinson, *Nat. Mater.*, 2013, **12**, 1064–1071, DOI: 10.1038/nmat3772.

D. Needham and R. M. Hochmuth, *J. Biomech. Eng.*, 1990, **112**, 269–276, DOI: 10.1115/1.2891184.

A. Yeung and E. Evans, *Biophys. J.*, 1989, **56**, 139–149.

D. S. Courson and R. S. Rock, *J. Biol. Chem.*, 2010, **285**, 26350–26357, DOI: 10.1074/jbc.M110.123117.

M. A. Tsai, R. S. Frank and R. E. Waugh, *Biophys. J.*, 1993, **65**, 2078–2088.

E. Shojaei-Baghini, Y. Zheng and Y. Sun, *Ann. Biomed. Eng.*, 2013, **41**, 1208–1216, DOI: 10.1007/s10439-013-0791-9.

T. Q. P. Uyeda, Y. Iwadate, N. Umeki, A. Nagasaki and S. Yumura, *PLoS One*, 2011, **6**, e26200, DOI: 10.1371/journal.pone.0026200.
O. Thoumine, O. Cardoso and J. J. Meister, *Eur. Biophys. J.*, 1999, **28**, 222–234, DOI: 10.1007/s002490050203.
D. P. Theret, M. J. Levesque, M. Sato, R. M. Nerem and L. T. Wheeler, *J. Biomech. Eng.*, 1988, **110**, 190–199.
L. Yong Sheng and C. Wei Yi, *Sci. China, Ser. G: Phys., Mech. Astron.*, 2013, **56**, 2208–2215, DOI: 10.1007/s11433-013-5258-3.
M. Sato, D. P. Theret, L. T. Wheeler, N. Ohshima and R. M. Nerem, *J. Biomech. Eng.*, 1990, **112**, 263–268, DOI: 10.1115/1.2891183.
E. H. Zhou, F. D. Martinez and J. J. Fredberg, *Nat. Mater.*, 2013, **12**, 184–185.
R. Transontay, D. Needham, A. Yeung and R. M. Hochmuth, *Biophys. J.*, 1991, **60**, 856–866.
G. R. Plaza, N. Marí, B. G. Gálvez, A. Bernal, G. V. Guinea, R. Daza, J. Pérez-Rigueiro, C. Solanas and M. Elices, *Phys. Rev. E: Stat., Nonlinear, Soft Matter Phys.*, 2014, **90**, 052715, DOI: 10.1103/PhysRevE.90.052715.
T. Q. P. Uyeda, P. D. Abramson and J. A. Spudich, *Proc. Natl. Acad. Sci. U. S. A.*, 1996, **93**, 4459–4464, DOI: 10.1073/pnas.93.9.4459.
J. A. Spudich, *Nat. Rev. Mol. Cell Biol.*, 2001, **2**, 387–392, DOI: 10.1038/35073086.
E. M. Darling, M. Topel, S. Zauscher, T. P. Vail and F. Guilak, *J. Biomech.*, 2008, **41**, 454–464, DOI: 10.1016/j.jbiomech.2007.06.019.
M. L. Rodriguez, P. J. McGarry and N. J. Sniadecki, *Appl. Mech. Rev.*, 2013, **65**, 060801, DOI: 10.1115/1.4025355.
G. I. Zahalak, W. B. Mcconnaughey and E. L. Elson, *J. Biomech. Eng.*, 1990, **112**, 283–294, DOI: 10.1115/1.2891186.
C. Veigel, J. E. Molloy, S. Schmitz and J. Kendrick-Jones, *Nat. Cell Biol.*, 2003, **5**, 980–986, DOI: 10.1038/ncb1060.
M. Kovacs, K. Thirumurugan, P. J. Knight and J. R. Sellers, *Proc. Natl. Acad. Sci. U. S. A.*, 2007, **104**, 9994–9999, DOI: 10.1073/pnas.0701181104.
G. R. Plaza and T. Q. P. Uyeda, *Soft Matter*, 2013, **9**, 4390–4400, DOI: 10.1039/c3sm27867k.
G. R. Plaza, *Phys. Rev. E: Stat., Nonlinear, Soft Matter Phys.*, 2010, **82**, 031902, DOI: 10.1103/PhysRevE.82.031902.
F. Nakamura, T. P. Stossel and J. H. Hartwig, *Cell Adhesion & Migration*, 2011, **5**, 160–169, DOI: 10.4161/cam.5.2.14401.
A. J. Ehrlicher, F. Nakamura, J. H. Hartwig, D. A. Weitz and T. P. Stossel, *Nature*, 2011, **478**, 260–263, DOI: 10.1038/nature10430.
R. S. Hock and J. S. Condeelis, *J. Biol. Chem.*, 1987, **262**, 394–400.
R. K. Meyer and U. Aebi, *J. Cell Biol.*, 1990, **110**, 2013–2024, DOI: 10.1083/jcb.110.6.2013.
J. Ylanne, K. Scheffzek, P. Young and M. Saraste, *Structure*, 2001, **9**, 597–604, DOI: 10.1016/S0969-2126(01)00619-0.
J. M. Ferrer, H. Lee, J. Chen, B. Pelz, F. Nakamura, R. D. Kamm and M. J. Lang, *Proc. Natl. Acad. Sci. U. S. A.*, 2008, **105**, 9221–9226, DOI: 10.1073/pnas.0706124105.
W. H. Goldmann and G. Isenberg, *FEBS Lett.*, 1993, **336**, 408–410, DOI: 10.1016/0014-5793(93)80847-N.
H. Miyata, R. Yasuda and K. Kinosita, *Biochim. Biophys. Acta, Gen. Subj.*, 1996, **1290**, 83–88, DOI: 10.1016/0304-4165(96)00003-7.
L. Rognoni, J. Stigler, B. Pelz, J. Ylaenne and M. Rief, *Proc. Natl. Acad. Sci. U. S. A.*, 2012, **109**, 19679–19684, DOI: 10.1073/pnas.1211274109.
Y. Lad, T. Kiema, P. Jiang, O. T. Pentikaeinen, C. H. Coles, I. D. Campbell, D. A. Calderwood and J. Ylaenne, *EMBO J.*, 2007, **26**, 3993–4004, DOI: 10.1038/sj.emboj.7601827.
U. Pentikainen and J. Ylanne, *J. Mol. Biol.*, 2009, **393**, 644–657, DOI: 10.1016/j.jmb.2009.08.035.
L. Eichinger, B. Koppel, A. A. Noegel, M. Schleicher, M. Schliwa, K. Weijer, W. Witke and P. A. Janmey, *Biophys. J.*, 1996, **70**, 1054–1060.
F. Rivero, R. Furukawa, M. Fechheimer and A. A. Noegel, *J. Cell Sci.*, 1999, **112**, 2737–2751.
M. Sussman, *Methods Cell Biol.*, 1987, **28**, 9–29.
K. M. Ruppel, T. Q. P. Uyeda and J. A. Spudich, *J. Biol. Chem.*, 1994, **269**, 18773–18780.
T. Q. P. Uyeda and J. A. Spudich, *Science*, 1993, **262**, 1867–1870, DOI: 10.1126/science.8266074.